

Deterministic single shot and multiple shots bulk damage thresholds for doped and undoped, crystalline and ceramic YAG

Binh T. Do*

Sandia National Laboratories, Albuquerque, NM 87105

Arlee V. Smith

AS-Photonics, Albuquerque, NM 87112

*Current address: Ball Aerospace Technologies Corporation, NM 87106

Abstract

We measured the single-shot and multiple-shot damage thresholds of pure and Nd-doped ceramic Yttrium Aluminum Garnet (YAG), and of pure, Nd-doped, Cr-doped, and Yb-doped crystalline YAG. We used 9.9 ns, single-longitudinal-mode, TEM₀₀ pulses tightly focused inside the ceramic and crystalline YAG. The 8 microns radius of the focal spot was measured using surface third harmonic generation. With this tight focus the damage threshold powers for both the ceramic and crystalline YAG were below the SBS threshold, and the effect of self focusing was small.

We found the single-shot and multiple-shots damage thresholds to be deterministic. The single-shot damage of YAG occurs on the trailing edge of the laser pulse, in contrast to fused silica in which damage always occurs at the peak of the laser pulse. However, the multiple-shot damage threshold of YAG occurs at the peak of the n^{th} laser pulse.

We find the damage thresholds of doped and undoped, ceramic and crystalline YAG range from 1.1 to 2.2 kJ/cm². We also report some damage morphologies in YAG.

I. Introduction

Crystalline YAG has been an important laser material for several decades. Recently, ceramic YAG technology has matured to the point that its optical quality is comparable to crystalline YAG. The optical damage thresholds of these two materials are important in the development and applications of high power lasers because laser induced damage imposes an ultimate limit to system performance. However, there are few reports on the damage threshold of YAG. Bisson *et al.* [1] reported that for nanosecond pulses varying the fluence from 110 to 250 J/cm² caused the damage probability to rise from 0 % to 100

% for undoped crystalline YAG. For undoped ceramic YAG, the corresponding fluence range was 105 - 245 J/cm². The damage threshold was claimed to be statistical and dependent on the focusing volume because the optical breakdown was thought to start from the seed electrons that were generated from the impurities in the sample. However, as we showed in silica damage measurements, an apparent statistical behavior can be due to the statistical properties of the optical field from a multi longitudinal mode laser such as used by Bisson *et al.*

In this work, we used an injection seeded Nd:YAG laser, operating on a single longitudinal mode. By tightly spatially filtering the laser beam, we made its spatial mode very close to be TEM₀₀. We precisely measured the focal spot size by measuring the surface third harmonic signal. We also measured the laser power at breakdown. From that information, we were able to calculate the damage threshold irradiance and fluence. We will describe our experimental set-up and technique in part II, and we will discuss our experimental results on the optical breakdown processes in crystalline and ceramic YAG in part III. We will also briefly discuss the broadband light emitted from the optical breakdown region in part IV. Finally, we will show the damage morphologies in part V and a conclusion in part VI.

II. Experimental set-up and technique

II.1. Properties of optical breakdown

A laser can excite electrons into the conduction band by tunneling ionization, by multiphoton ionization, and by impact ionization. When the free electron density reaches the critical density, then the plasma frequency is equal to the laser frequency,

$$\omega_p^2 = \frac{e^2 n}{m^* \epsilon \epsilon_0} = \omega_{laser}^2, \quad [\text{Eq. 1}]$$

where e is the electron charge, n is the free electron density, m^* is the effective electron mass, ϵ is the relative permittivity of the medium, and ϵ_0 is the free space permittivity. For our 1.064 μm laser the critical density of free electrons in undoped crystalline YAG is $3.26 \times 10^{21}/\text{cm}^3$.

When optical breakdown begins, the following phenomena occur simultaneously [2].

a. A drastic decrease in the transmitted laser power occurred as the incident laser pulse is reflected, absorbed, and scattered by the dense plasma created by optical breakdown at the focal region.

b. The generation of a high-density plasma in the focusing region creates a bright flash of white light.

c. At the onset of the optical breakdown, the dense plasma started to scatter light from a probe beam.

In our experimental set-up, we used fast phototubes to record the incident and transmitted pump beams, a photomultiplier tube to record the broadband light generated at the optical region, and a screen to display the transmitted probe beam.

II.2. Experimental set-up

We used a single-longitudinal-mode, injection-seeded, Q-switched YAG laser operating at 1.064 μm . The temporally smooth pulse is repeatable with a 1% pulse-to-pulse amplitude variation. In contrast, a multiple-longitudinal-mode laser produces non reproducible pulses comprised of numerous short temporal spikes. In order to extract a single laser pulse or a set number of laser pulses from our 10 pps laser while keeping the laser oscillator locked to the seed laser, we used a beam shutter synchronized to the Q-switch signal which opened for 40 msec before the first pulse and closed at 40 msec after the last pulse. We varied the pulse energy using a half wave plate and a high-energy cube polarizer. We used a 200- μm -diameter wire die and an adjustable iris to spatially filter the laser beam to make it a close approximation to a TEM_{00} profile. We also used two fast phototubes (Hamamatsu, R1193U-01) to record the incident and transmitted pump beams, and a photomultiplier (Hamamatsu, 1P28) to record the broadband light emitted from the optical breakdown region. The transmitted HeNe probe beam aligned with the high power beam was displayed on a screen after the sample. The sample was mounted on a motorized 3-dimensional translation stage, and we focused the pump beam into the sample with a 1-inch focal length, best form lens manufactured by CVI. The experimental set-up is shown in Fig.1.

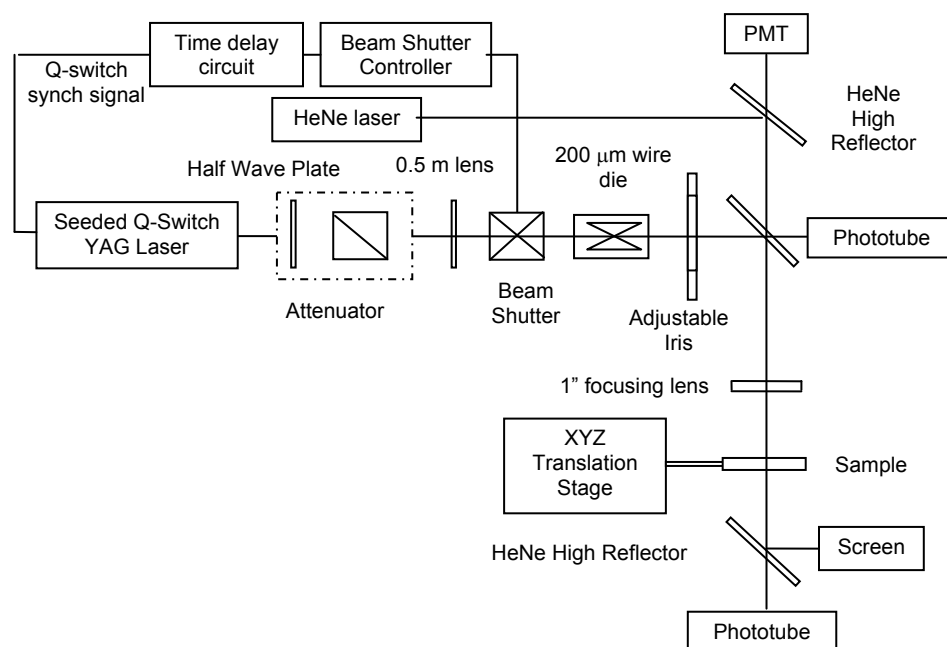


Fig. 1: Experimental set-up

II.3. Spatial and temporal profiles of laser pulses

II.3a. Spatial beam profile measurement

Figure 2 shows the spatial profile of the beam before going through the focusing lens. The spatial profile is close to the TEM_{00} mode, ensuring that it focuses to a nearly diffraction-limited spot size without hot spots.

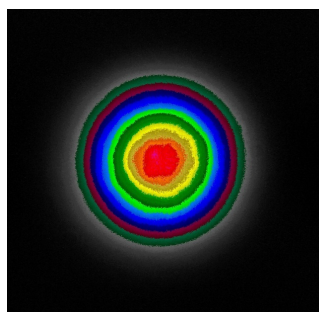


Fig. 2: The spatial profile of our laser beam before going to the focusing lens.

II.3b. Temporal profile of laser pulses

The temporal profile of the high power 1064 nm pulse is shown in Fig. 3.

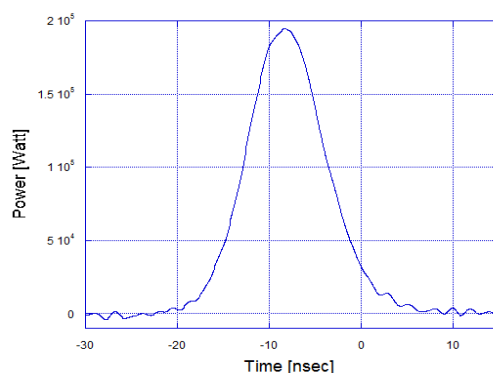


Fig. 3: The temporal profile of our laser pulse, the FWHM is about 9.9 nsec.

If we unseeded our laser, then it would run multimode. The gain bandwidth of YAG is about 30 GHz, and the free spectral range of our laser was 250 MHz. However, not all of the cavity modes under the gain curve actually are above the lasing threshold. If we assume that there were eight equally spaced modes under the gain curve that lased with random (uncorrelated) phases, then these modes would interfere with each other to produce an output pulse which consisted of a multitude of high-intensity spikes as shown in Fig. 4. The power of the highest spike can be four times higher than the maximum power of the seeded pulse of the same energy. The lasing bandwidth of Nd:YAG is 30 GHz. From the uncertainty relation $\Delta t \Delta \omega \geq 1$, we can estimate the duration of these high intensity spikes to be about 15 psec.

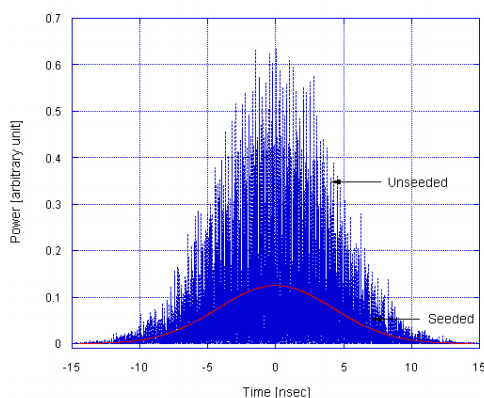


Fig. 4: The simulated temporal profile of an unseeded laser beam.

If the damage mechanism is nonlinear in power, the damage threshold fluence of a multimode pulse can be smaller than that of the single-longitudinal-mode laser beam. Moreover, the temporal profile of a multimode laser beam varies from pulse to pulse, so

the optical damage fluence can appear to be statistical when using an unseeded laser but deterministic when using a seeded laser.

II.3c. Method of measuring and locating the beam waist

In this experiment, we wished to measure the laser fluence at breakdown, and also study the morphology of the material damage created by optical breakdown. This study can be precise only if we knew the exact location and the size of the focal spot in our sample.

We found the location and the size of the laser beam waist by measuring the surface third harmonic signal generated by the broken symmetry at the air-sample interface. The bulk third harmonic signal exists, but it is much weaker than the surface third harmonic signal [3]. The surface third harmonic pulse energy is

$$Energy^{(3\omega)} \approx \int_0^\infty \int_0^{2\pi} I_w^3 \exp\left(-6 * \frac{r^2}{w^2}\right) r d\theta dr \approx \frac{1}{w^4}, \quad [\text{Eq. 2}]$$

where w is the beam radius at $1/e^2$ on the surface of the sample,

$$w^2 = w_0^2 \left(1 + \frac{(z - z_0)^2 \lambda^2}{(\pi w_0^2)^2} \right), \quad [\text{Eq. 3}]$$

w_0 is the radius of the beam waist, and z_0 is the location of the beam waist. Fig. 5 showed the surface third harmonic signal with respect to the nominal location of the sample.

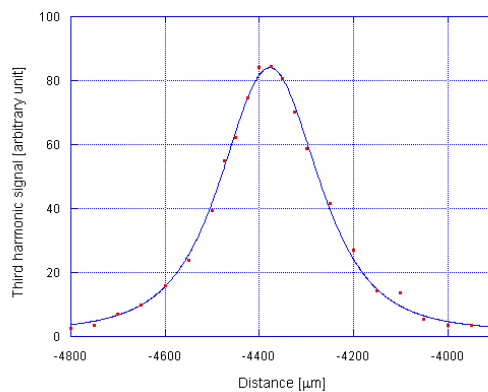


Fig. 5: Surface third harmonic signal as a function the nominal location of the sample. The dots are measured points and the solid line is a least-square fit to $1/w^4$.

The surface third harmonic signal is a maximum when the beam waist coincides with the sample surface. From our fit to $1/w^4$, we obtain the focus spot size of $w_0 = 8.1 \pm 0.1$

μm . Additionally, we determine z_0 so we can position the focal spot a certain distance into the sample.

III b. Laser induced damage thresholds in un-doped crystalline and ceramic YAG

The dimension of the YAG samples was 0.5" in diameter and 0.5" in thickness. The focusing spot size was 3.6 mm behind the front surface. We measured single-shot and cumulative multiple-shot damage thresholds at a 1 Hz repetition rate for un-doped crystalline and ceramic YAG.

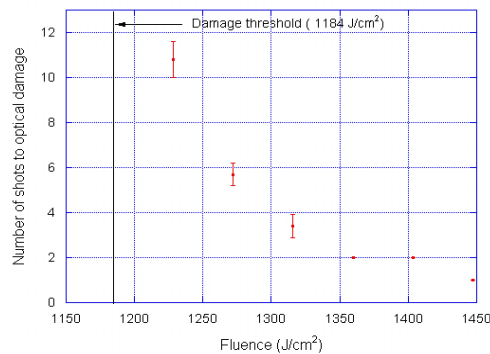


Fig. 6: Single shot and multiple shot damage thresholds of undoped crystalline YAG for linearly polarized light, 9.9 nsec FWHM pulse duration.

Fig. 6 shows the thresholds for un-doped crystalline YAG for linearly polarized light. The single-shot damage threshold fluence was $1447 \text{ J}/\text{cm}^2$; the two-shot fluence range included 1404 and $1360 \text{ J}/\text{cm}^2$. At $1316 \text{ J}/\text{cm}^2$ damage occurred on either the third or fourth pulse; at $1272 \text{ J}/\text{cm}^2$ damage occurred on either the fifth, sixth, or the seventh pulse. When the fluence was reduced to $1184 \text{ J}/\text{cm}^2$ damage did not occur no matter how many pulses we applied to a single spot. We call this the damage threshold in Fig. 6. We believe a more detailed study could identify more precisely the locations of the steps in this figure. Note that these fluences are not corrected for self focusing.

For the undoped ceramic YAG, the behavior was qualitatively similar to that for undoped crystalline YAG, as shown in Fig. 7. Note that the $1564 \text{ J}/\text{cm}^2$ damage threshold for undoped ceramic YAG is higher than the $1184 \text{ J}/\text{cm}^2$ threshold of undoped crystalline YAG. The ratio of single pulse threshold to multi pulse threshold is also considerably larger.

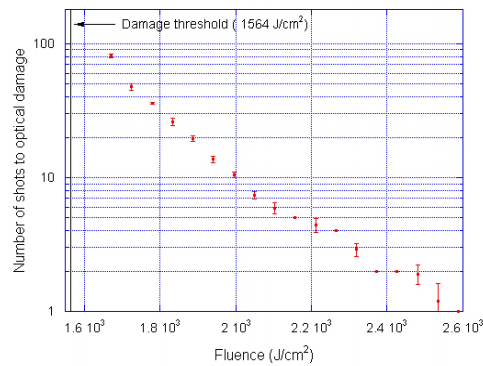
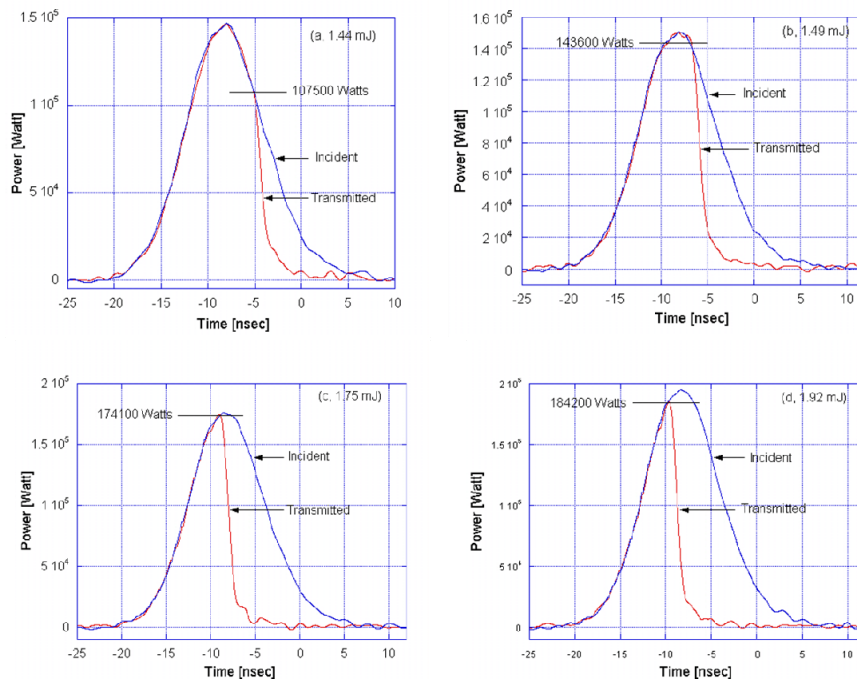


Fig. 7: Damage thresholds for undoped ceramic YAG for linearly polarized light.

We also recorded profiles of the incident and transmitted pulses near the single-shot threshold and at higher pulse energy. Fig. 8 shows such profiles for several pulse energies. The power at the time of breakdown is indicated on the plots.

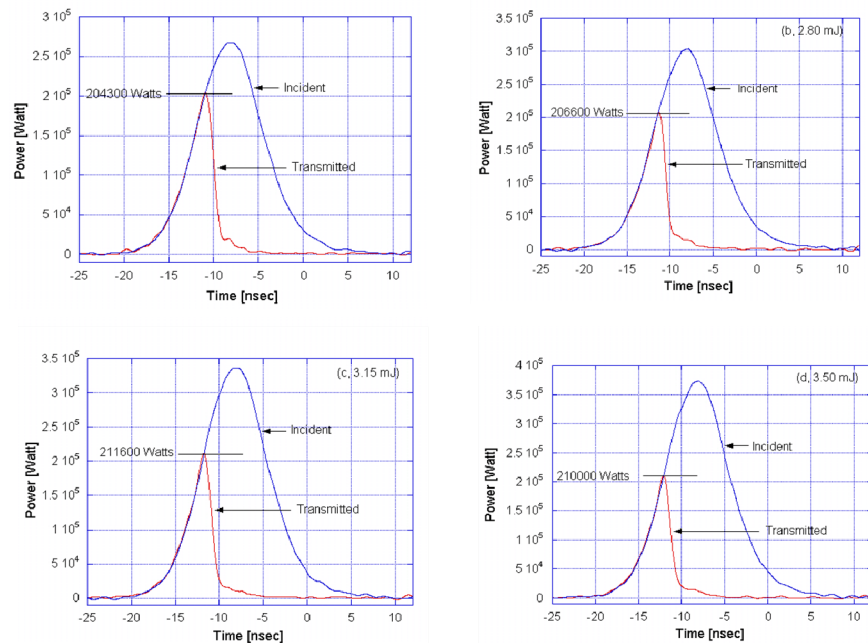


Figs. 8: Temporal profiles of the incident and transmitted pulses at different incident pulse energies in undoped crystalline YAG for single shot damage, (a) 1.44 mJ (b) 1.49 mJ, (c) 1.75 mJ, and (d) 1.92 mJ.

The pulse energy of 1.44 mJ corresponds to the single shot threshold. For this energy, breakdown occurred on the falling edge of the pulse at 107.5 kW, compared with the peak power of 147.1 kW. At an incident energy of 1.49 mJ (Fig. 8b), well above the single pulse threshold, breakdown still occurs on the falling edge of the pulse at 143.6

kW, but nearer to the peak. Figs. 8c, and 8d show the traces of incident and transmitted beams at still higher energies of 1.75 mJ and 1.92 mJ where breakdown occurs on the rising edge of the pulse at 174.1 and 184.2 kW, respectively. Clearly, in undoped crystalline YAG, breakdown is caused by a cumulative process, and it occurs at different powers that depend on the incident pulse energy.

We increased the pump energy still further to 2.45 mJ and 2.80 mJ, and found breakdown occurred on the rising edge of the pulse, and at the higher laser powers of 204.3 and 206.6 kW, respectively. However, when the pump energy was 3.15 mJ and 3.50 mJ, the breakdown occurred at 211.6 and 210 kW, respectively. The temporal profiles of the incident and transmitted pulses at these pulse energies are shown in Figs. 9.



Figs. 9: Temporal profiles of incident and transmitted beams for undoped crystalline YAG at pulse energies of (a) 2.45mJ, (b) 2.80 mJ, (c) 3.15 mJ, and (d) 3.50 mJ.

We also measured the time at breakdown for energies exceeding the single pulse threshold, defined from the peak of the incident pulse to the start of the optical breakdown. If the breakdown occurred on the rising edge of the incident pulse, the time is negative. Fig. 10 shows the measured breakdown times.

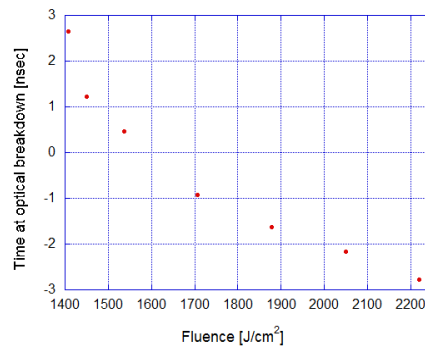


Fig. 10: Breakdown time in the undoped crystal YAG as a function of laser fluence.

We also measured the pulse energy up to the time of breakdown as a function of the incident pulse energy for energies exceeding the single pulse threshold (see Fig. 11).

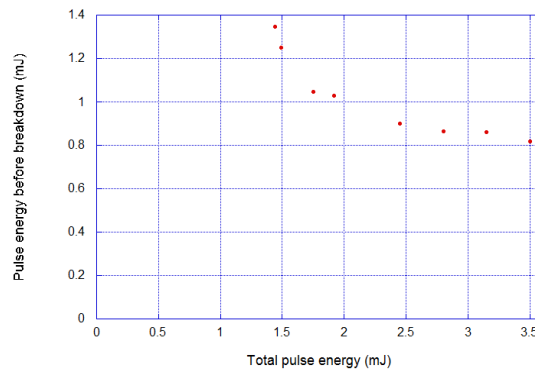
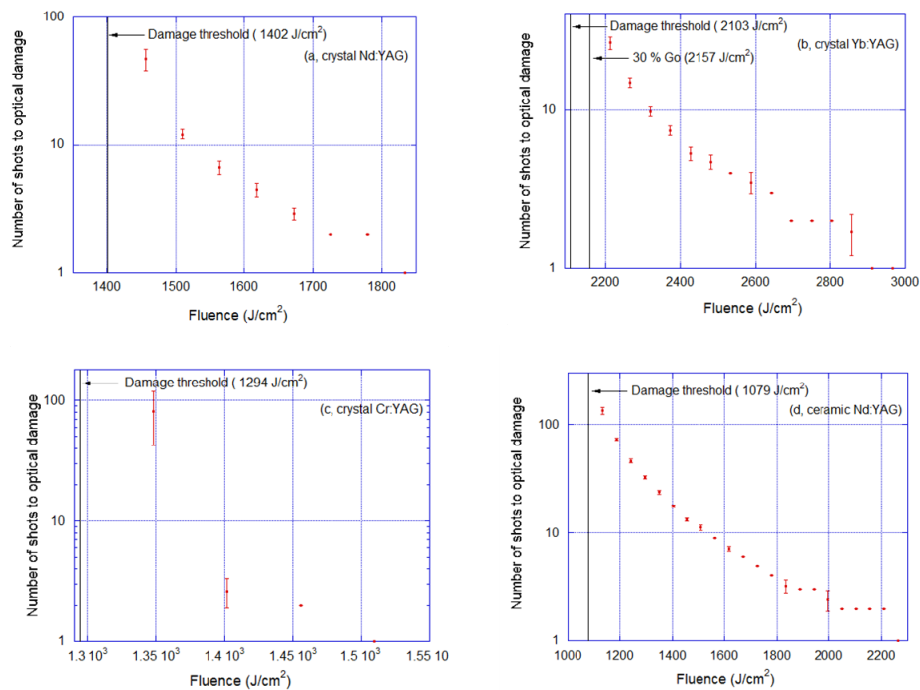


Fig. 11: Laser pulse energy before breakdown versus incident pulse energy

At lower energy where multiple-shots are required, breakdown always occurs at the peak of the pulse.

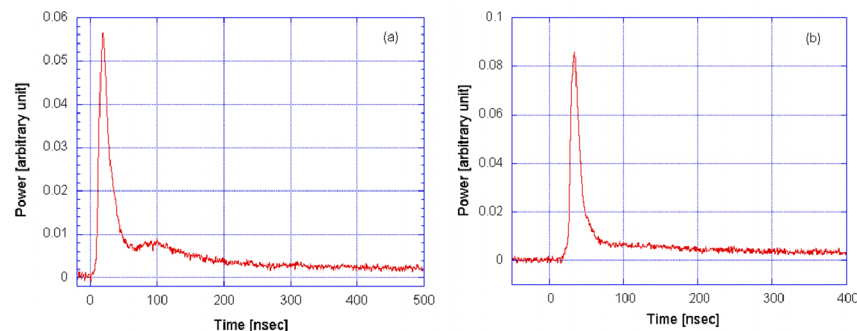
The single shot and multiple shot damage thresholds of doped crystalline and ceramic YAG are compared in Figs. 12 (a), (b), (c), and (d). The thresholds of the doped samples behaved qualitatively similar to the undoped samples.



Figs. 12: Single and multiple pulse damage thresholds of Nd, Yb, and Cr doped crystalline and ceramic YAG for linearly polarized, 9.9 nsec FWHM pulses.

IV. Broadband light emission from breakdown in undoped crystalline and ceramic YAG

One signature of optical breakdown is broadband light emitted from the focal region. The temporal profile of this broadband light is different in YAG than in fused silica [4]. Fig. 13 shows temporal profiles of the broadband light emitted by undoped crystalline and ceramic YAG.



Figs. 13: Temporal profiles of the broadband light emitted from the focal region in undoped (a) crystalline and (b) ceramic YAG.

The broadband light from undoped crystalline YAG consisted of a short pulse and a broad pulse. The FWHM of the short pulse was about 20 nsec. A possible explanation is that at the beginning of breakdown the electron density in the plasma region exceeds the critical density and radiative recombination of electrons and matrix could emit the short pulse. Non radiative recombination could heat the focal region and its surroundings on a longer time scale, and the heated zone could radiate as a black body, producing the broader pulse.

V. Optical damage morphology

We also studied damage morphologies in undoped crystalline YAG. We cut and polished the damaged samples along the propagation direction of the pump beam, to obtain the side views of the damage. The end views were not very informative. Fig. 14 shows two damaged spots created at different pulse energies. The damage on the right was generated by a pulse only slightly above the single-shot threshold, and the damage on the left was generated by a pulse with energy 30% higher. The dashed line indicates the location of the focal waist. The size of the white dot gives an indication of the uncertainty ($\pm 10 \mu\text{m}$) in the location of the focusing spot, and the two arcs along the propagating direction represent the focusing beam size. Breakdown probably starts at the focus, where the irradiance is highest. The optical damage shown in Fig. 14 were very reproducible.

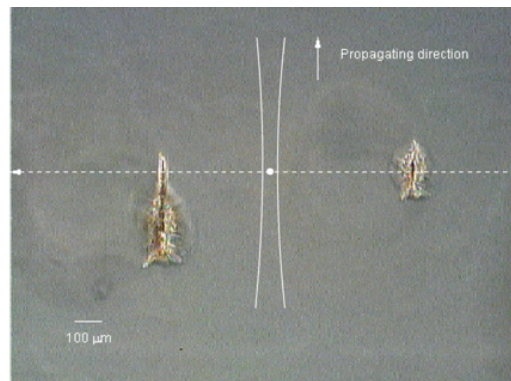


Fig. 14: Damage morphologies in undoped crystalline YAG

IV. Conclusion

We have shown that the single-shot and multiple-shot optical damage thresholds in doped and un-doped crystalline and ceramic YAG for a 9.9 ns (FWHM) pulse with an

8.1- μm beam radius are deterministic. We could observe the deterministic behaviour of these damage thresholds because we used a well controlled laser with a single longitudinal mode and a spatial mode that is close to TEM_{00} , and a pulse energy that varies 1% from pulse to pulse. If we had used a multi-longitudinal mode laser, the damage thresholds of YAG probably would have appeared to be statistical due to the statistical nature of the light pulses rather than to an inherently statistical damage process.

The damage threshold for undoped ceramic YAG is higher than that for undoped crystalline YAG. However, the damage threshold of ceramic Nd:YAG is lower than that of crystalline Nd:YAG

In single-pulse damage breakdown can occur on either side of the laser pulse depending on the incident pulse energy. In multiple-shot damage the breakdown always occurred at the peak of the pulse. We also studied the white light emitted by the breakdown and its temporal profile may provide information about the modification process at the focus. Our result also showed that the damage morphologies in YAG were very reproducible.

References

1. J. Bisson, Y. Feng, A. Shirakawa, H. Yoneda, J. Lu, H. Yagi, T. Yanagitani, K. Ueda, "Laser damage threshold of ceramic YAG", Japan J. Appl. Phys., 42, L1025-L1027 (2003).
2. N. Bloembergen, "Laser-induced electric breakdown in solids", IEEE J. Quantum. Electron, QE-10, 375-386 (1974).
3. T. Tsang, "Optical third-harmonic generation at interfaces", Phys. Rev. A, 52, 4116-4125 (1995).
4. A. Smith, B. Do, and M. Soderlund, "Nanosecond laser-induced breakdown in pure and Yb^{3+} doped fused silica", Laser-Induced Damage in Optical Materials: 2006. Edited by Exarhos, Gregory J.; Guenther, Arthur H.; Lewis, Keith L.; Ristau, Detlev; Soileau, M. J.; Stolz, Christopher J.. Proc. SPIE, Volume 6403, 640321.1-640321.12 (2007).

Deterministic single shot and multiple shots bulk damage thresholds for doped and undoped, crystalline and ceramic YAG

[7504-78]

Questions and Answers

Q. Did you mention how many samples you evaluated? What was your sample set size?

A. Quite a few. For each we looked at many. For crystalline YAG we had about ten samples or so. Then we did the statistics on many sites. They all behaved the same way.

Q. My question was if you noticed a difference in spread in the values between the crystalline YAG and the ceramic YAG? Did you notice any inconsistencies in the material grade in ceramic versus crystalline?

A. In ceramic YAG, the grain size is about 20 microns or so, so perhaps the grain size of ceramic YAG gives a contribution. But, that is just my speculation. I don't know. I just report the result.

Q. But, sample to sample you did not see a large variation?

A. For ceramic YAG, we did not see a large variation.